Threshold scans in diffractive W pair production via QED processes at the LHC

M. Boonekamp* and C. Royon†
Service de physique des particules, CEA/Saclay, 91191 Gif-sur-Yvette cedex, France

J. Cammin‡
University of Rochester, New York, USA

R. Peschanski§
Service de physique théorique, CEA/Saclay, 91191 Gif-sur-Yvette cedex, France¶

We propose a new set of measurements which can be performed at the LHC using roman pot detectors. This new method is based on exploiting excitation curves to measure kinematical properties of produced particles. We illustrate it in the case of central diffractive W pair production.

I. INTRODUCTION

We propose a new method to measure heavy particle properties via double photon exchange at the LHC. In this category of events, the heavy objects are produced in pairs, whereas the beam particles often leave the interaction region intact, and can be measured using very forward detectors.

If the events are *exclusive*, *i.e.*, if no other particles are produced in addition to the pair of heavy objects and the outgoing protons, the proton measurement gives access to the photon-photon centre-of-mass, and the dynamics of the hard process can be accurately studied. In particular, one can observe the threshold excitation and attempt to extract the mass of the heavy particle, or study its (possibly energy-dependent) couplings by measuring cross-sections and angular distributions [1]. As examples of this approach, we give a detailed account of the W boson measurement at production threshold. The method can easily be extended to other heavy objects in exclusive production.

The Letter is organised as follows. We start by giving the theoretical formulation of $\mathrm{W^+W^-}$ production (via QED). We then describe the event generation, the simulation of detector effects, and the cuts used in the analysis. The following part of the paper describes in detail the threshold scan method, in a twofold version ("turn-on"and "histogram" fits), and its application to the W boson measurements.

II. THEORETICAL FORMULATION OF W PAIR QED PRODUCTION

The QED process rates are obtained from the following cross section formula

$$d\sigma_{(\mathrm{pp}\to\ \mathrm{p\ W^+W^-p})} = \hat{\sigma}_{\gamma\gamma\to\mathrm{W^+W^-}}\ dn_1^\gamma\ dn_2^\gamma\ ,$$

where the Born $\gamma\gamma \to \mathrm{W^+W^-}$ cross-section reads [2]

$$\hat{\sigma}_{\gamma\gamma\to\mathrm{W^+W^-}} = \frac{8\pi\alpha^2}{M_{\mathrm{WW}}^2}\left\{\frac{1}{t}\left(1+\frac{3}{4}t+3t^2\right)\Lambda - 3t(1-2t)\ln\left(\frac{1+\Lambda}{1-\Lambda}\right)\right\}, \tag{1}$$

with

$$t = \frac{m_{\mathrm{W}}^2}{M_{\mathrm{WW}}^2}\ , \qquad \Lambda = \sqrt{1-4t}\ , \tag{2}$$

where M_{WW} is the total $\mathrm{W^+W^-}$ mass. The photon fluxes dn^γ are given by [3]

$$dn^\gamma = \frac{\alpha}{\pi}\frac{\omega}{\omega}\left(1-\frac{\omega}{E}\right)\left[\phi\left(\frac{q^2_{max}}{q_0^2}\right) - \phi\left(\frac{q^2_{min}}{q_0^2}\right)\right]\ , \tag{3}$$

¶ URA 2306, unité de recherche associée au CNRS.

*Electronic address: boon@hep.saclay.cea.fr
†Electronic address: royon@hep.saclay.cea.fr
‡Electronic address: cammin@fnal.gov
§Electronic address: pesch@spht.saclay.cea.fr

where

$$\phi\,(x) \equiv (1+ay)\left[\ln\left(\frac{x}{1+x}\right)+\Sigma_{k=1}^{3}\frac{1}{k(1+x)^k}\right]-\frac{(1-b)y}{4x(1+x)^3+c(1+\frac{1}{4}y)}\left[\ln\left(\frac{2+2x-b}{1+x}\right)+\Sigma_{k=1}^{3}\frac{b^k}{k(1+x)^k}\right]\ , \quad (4)$$

and

$$q_0^2 \sim 0.71\ \mathrm{GeV}^2\ \ ;\ y=\frac{\omega^2}{E(E-\omega)}\ \ ;\ a\sim 7.16\ \ ;\ b\ \ \sim -3.96\ \ ;\ c\sim 0.028\ , \quad (5)$$

in the usual dipole approximation for the proton electromagnetic form factors. ω is the photon energy in the laboratory frame, q^2 the modulus of its mass squared in the range

$$\left[q^2_{min},\ q^2_{max}\right] \equiv \left[\frac{m^2\omega^2}{E(E-\omega)}\ ,\frac{t_{max}}{q_0^2}\right]\ , \quad (6)$$

where E and m are the energy and mass of the incident particle and $t_{max} \equiv (m_{\mathrm{W}}^2/M_{\mathrm{WW}}^2)_{max}$ is defined by the experimental conditions.

The QED cross section $d\sigma(\mathrm{pp} \rightarrow\ \mathrm{p\ W^+W^-p})$ is a theoretically clear prediction. One should take into account however, two sources of correction factors. One is due to the soft QCD initial state radiation between incident protons which could destroy the large rapidity gap of the QED process. It is present but much less pronounced than for the rapidity gap survival for a QCD hard process (see the discussion in the next subsections), thanks to the large impact parameter implied by the QED scattering. The second factor is the QCD $\mathrm{gg} \rightarrow \mathrm{W^+W^-}$ exclusive production via higher order diagrams. This remains to be evaluated. In standard recently (non diffractive) production [4], it is small. The similar calculation for the diffractive $\mathrm{W^+W^-}$ production by comparison with the QED process is outside the scope of our paper but deserves to be studied together with the "inclusive" background ($\mathrm{W^+W^-}$+hadrons) it could generate.

A. Rapidity Gap Survival

In order to select exclusive diffractive states, such as for $\mathrm{W^+W^-}$ (QED), it is required to take into account the corrections from soft hadronic scattering. Indeed, the soft scattering between incident particles tends to mask the genuine hard diffractive interactions at hadronic colliders. Starting with the "hard" scattering amplitude $\mathcal{A}_{(\mathrm{WW})}$, the formulation of this correction [5, 6] consists in considering its convolution with a soft S-matrix elemeny S which reflects the small "rapidity gap survival" factor due to the soft radiation always present when two initial hadrons collide [5]. One writes

$$\mathcal{A}(p_{T1},p_{T2},\Delta\Phi) = \{1+\mathcal{A}_{SP}\}\times\mathcal{A}_{(\mathrm{WW,t\bar{t}})} \equiv \mathcal{S}\times\mathcal{A}_{(\mathrm{WW,t\bar{t}})} = \int d^2\mathbf{k}_T\ \mathcal{S}(\mathbf{k}_T)\ \mathcal{A}_{(\mathrm{WW,t\bar{t}})}(\mathbf{p}_{T1}-\mathbf{k}_T,\mathbf{p}_{T2}+\mathbf{k}_T)\ , \quad (7)$$

where $\mathbf{p}_{T1,2}$ are the transverse momenta of the outgoing $p,\bar{p}$ and $\Delta\Phi$ their azimuthal angle separation. $\mathbf{k}_T$ is the intermediate transverse momentum integrated out by the convolution.

The correction for the QED process is present but much less pronounced than for the rapidity gap survival for a QCD hard process, thanks to the large impact parameter implied by the QED scattering. In a specific model [7] the correction factor has been evaluated to be of order 0.9 at the LHC for $\gamma\gamma \rightarrow \mathrm{H}$ and by contrast, 0.03 for the QCD exclusive diffractive processes at the LHC.

III. EXPERIMENTAL CONTEXT

A. The DPEMC Monte Carlo

A recently developed Monte-Carlo program, `DPEMC` [8], provides an implementation of the $\mathrm{W^+W^-}$ events described above in the QED exchange modes. It uses `HERWIG` [9] as a cross-section library of hard QCD processes, and when required, convolutes them with the relevant pomeron densities. HERWIG is only used for parton sjowering and hadronisation for exclusive processes. The survival probabilities discussed in the previous section (0.9 for double photon exchange processes) have been introduced at generator level. The cross section at generator level for $\mathrm{W^+W^-}$ QED is found to be 55.9 fb for a m_{W} mass of 80.42 GeV after applying the survival probabilities.

B. Roman pot detector positions and resolutions

A possible experimental setup for forward proton detection is described in detail in [10]. We will only describe its main features here and discuss its relevance for the W boson and top quark masses measurements.

In exclusive QED processes, the mass of the central heavy object can be reconstructed using the roman pot detectors and tagging both protons in the final state at the LHC. It is given by $M^2 = \xi_1 \xi_2 s$, where ξ_i are the proton fractional momentum losses, and s the total center-of-mass energy squared [11]. In order to reconstruct objects with masses in the 160 GeV range (for W^+W^- events) in this way, the acceptance should be large down to ξ values as low as a few 10^{-3}. The missing mass resolution directly depends on the resolution on ξ, and should not exceed a few percent to obtain a good mass resolution.

These goals can be achieved if one assumes two detector stations, located at ~ 220 m, and ~ 420 m [10] from the interaction point. The ξ acceptance and resolution have been derived for each device using a complete simulation of the LHC beam parameters. The combined ξ acceptance is close to $\sim 60\%$ at low masses (at about twice m_W).

Our analysis does not assume any particular value for the ξ resolution. We will discuss in the following how the resolution on the W boson mass depends on the detector resolutions, or in other words, the missing mass resolution.

C. Experimental cuts

Let us summarise the cuts applied in the remaining part of the analysis. As said before, both diffracted protons are required to be detected in roman pot detectors.

The triggers which will be used for the W^+W^- events will be the usual ones at the LHC requiring in addition a positive tagging in the roman pot detectors.

The experimental offline cuts and their efficiencies have been obtained using a fast simulation of the CMS detector [12] as an example, the fast simulation of the ATLAS detector [12] leading to the same results. If we require at least one lepton (electron or muon) with a transverse momentum greater than 20 GeV and one jet with a transverse momentum greater than 20 GeV for W^+W^- to be reconstructed in the acceptance of the main detector in addition to the tagged protons, we get an efficiency of about 30% for W^+W^- events. We give the mass resolution as a function of luminosity in the following after taking into account these efficiencies. If the efficiencies are found to be higher, the luminosities have to be rescaled by this amount.

IV. THRESHOLD SCAN METHODS

A. Explanation of the histogram and turn-on fit methods

We study two different methods to reconstruct the mass of heavy objects double diffractively produced at the LHC. As we mentioned before, the method is based on a fit to the turn-on point of the missing mass distribution at threshold.

One proposed method (the "histogram" method) corresponds to the comparison of the mass distribution in data with some reference distributions following a Monte Carlo simulation of the detector with different input masses corresponding to the data luminosity. As an example, we can produce a data sample for 100 fb^{-1} with different W masses. For each Monte Carlo sample, a χ^2 value corresponding to the population difference in each bin between data and MC is computed. The mass point where the χ^2 is minimum corresponds to the mass of the produced object in data. This method has the advantage of being easy but requires a good simulation of the detector.

The other proposed method (the "turn-on fit" method) is less sensitive to the MC simulation of the detectors. The threshold scan is directly sensitive to the mass of the diffractively produced object (in the W^+W^- case for instance, it is sensitive to twice the W mass). The idea is thus to fit the turn-on point of the missing mass distribution which leads directly to the mass of the produced object, the W boson. Due to its robustness, this method is considered as the "default" one in the following.

To illustrate the principle of these methods and their achievements, we apply them to the W boson in the following, and present in detail the reaches at the LHC. They can be applied to other threshold scans as well.

B. W mass measurement using diffractive QED events

In this section, we will first describe the result of the "turn-on fit" method to perform a measurement of the W mass using diffractive QED events. The advantage of the W^+W^- processes is that they do not suffer from any theoretical

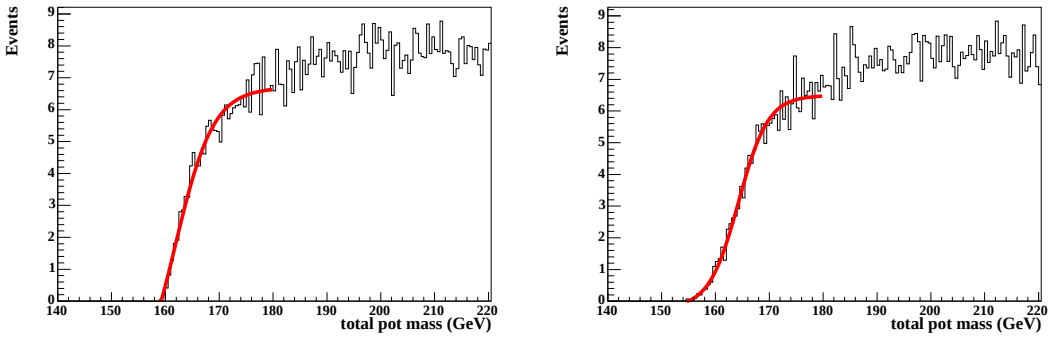

FIG. 1: Two examples of fits to missing mass reference distributions with a resolution of the roman pot detectors of 1 GeV (left) and 3 GeV (right). We see on these plots the principle and the accuracy of the "turn-on fits" to the MC at threshold. (Please note that the produced events were reweighted to a luminosity of 100 fb^{-1} in a standard way explaining why the statistical fluctuations are small.)

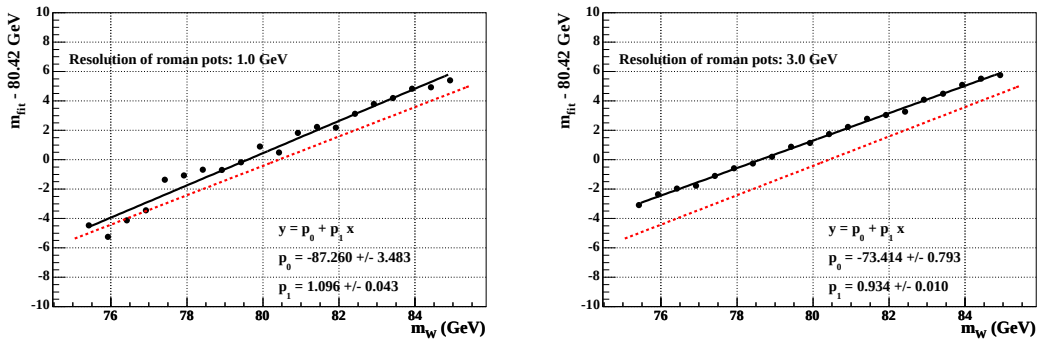

FIG. 2: Calibration curves (see text) for two different roman pot resolutions of 1 GeV (left) and 3 GeV (right). We notice that the calibration can be fitted to a linear function with good accuracy. The dashed line indicates the first diagonal to show the shift clearly.

uncertainties since this is a QED process. The W mass can be extracted by fitting a 4-parameter 'turn-on' curve to the threshold of the mass distribution (c.f. Ref. [13]):

$$\mathcal{F} = P_1 \cdot \left(\left[e^{-\frac{x-P_2}{P_3}} + 1 \right]^{-1} + P_4 \right). \tag{8}$$

P_1 is the amplitude, P_2 the inflexion point, P_3 the width of the turn-on curve, and P_4 is a vertical offset, x being the missing mass. With a detector of perfect resolution, P_2 would be equal to twice the W mass. However, the finite roman pot resolution leads to a shift between P_2 and $2m_{\mathrm{W}}$ which has to be established using a MC simulation of the detector for different values of its resolution. This shift is only related to the method itself and does not correspond to any error in data. For each value of the W input mass in MC, one has to obtain the shift between the reconstructed mass ($P_2/2$) and the input mass, which we call in the following the calibration curve. It is assumed for simplicity that P_2 is a linear function of m_{W}, which is a good approximation as we will see next. In order to determine the linear dependence between P_2 and m_{W}, calibration curves are calculated for several assumed resolutions of the roman pot detectors. The calibration points are obtained by fitting $\mathcal{F}$ to the mass distribution of high statistics samples (100 000 events) for several values of m_{W}. An example is given in Fig. 1 for two resolutions of the roman pot detectors. The difference between the fitted values of $P_2/2$ and the input W masses are plotted as a function of the input W mass and are then fitted with a linear function. To minimise the errors on the slope and offset, the difference $P_2/2 - 80.42$ GeV is plotted versus m_{W} (Fig. 2).

To evaluate the statistical uncertainty due to the method itself, we perform the fits with some 100 different "data" ensembles. For each ensemble, one obtains a different reconstructed W mass, the dispersion corresponding only to statistical effects. The expected statistical uncertainty on the actual measurement of the W mass in data is thus estimated with these ensemble tests for several integrated luminosities and roman pot resolutions. Each ensemble

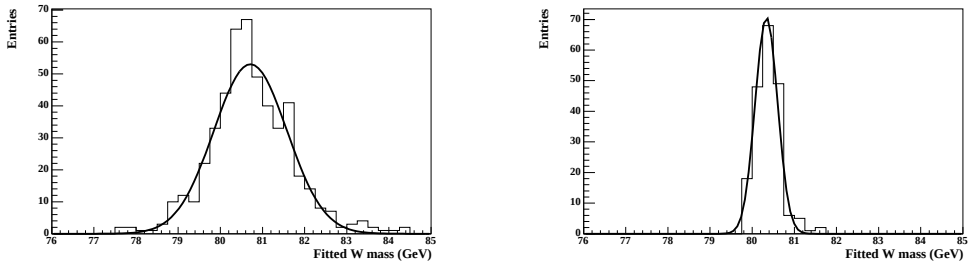

FIG. 3: Distribution of the fitted value of the W mass from ensemble tests. Left: corresponding to 150 fb^{-1}, right: corresponding to 300 fb^{-1}. We note the resolution obtained on the W mass for these two luminosities.

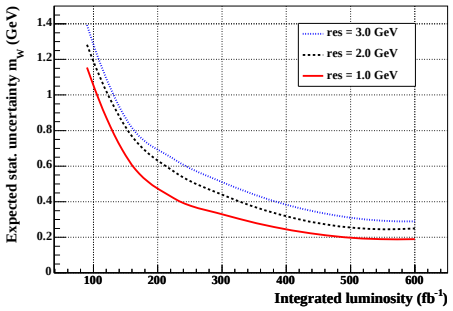

FIG. 4: Expected statistical uncertainty on the W mass as a function of luminosity for three different roman pot resolutions using the turn-on fit method.

contains a number of events that corresponds to the expected event yield for a given integrated luminosity, taking into account selection and acceptance efficiencies. The turn-on function $\mathcal{F}$ is fitted to each ensemble. Only the parameters P_1 and P_2 are allowed to float, P_3 and P_4 are fixed to the average values obtained from the fits for the calibration points.

In order to obtain the fitted estimate for the W mass, $m_{\mathrm{W}}^{\mathrm{fit}}$, in each ensemble, the fit value of P_2 is corrected with the calibration curve that corresponds to the roman pot resolution. For each resolution $m_{\mathrm{W}}^{\mathrm{fit}}$ is histogrammed as shown in Fig. 3. The distributions are fitted with a Gauss function where the width corresponds to the expected statistical uncertainty of the W mass measurement. Fig. 4 shows the expected precision as a function of the integrated luminosity for several roman pot resolutions. With 150 fb^{-1} the expected statistical uncertainty on m_{W} is about 0.65 GeV when a resolution of the roman pot detectors of 1 GeV can be reached. With 300 fb^{-1} the expected uncertainty on m_{W} decreases to about 0.3 GeV.

We notice of course that this method is not competitive to get a precise measurement of the W mass, which would require a resolution to be better than 30 MeV. However, this method can be used to align precisely the roman pot detectors for further measurements. A precision of 1 GeV (0.3 GeV) on the W mass leads directly to a relative resolution of 1.2% (0.4%) on ξ using the missing mass method.

Let us now present the result on the "histogram" method, which is an alternative approach to determine the W mass. The same high statistics templates used to derive the calibration curves are fitted directly to each ensemble (see Fig. 5 left). The χ^2 is defined using the approximation of poissonian errors as given in Ref. [14]. Each ensemble thus gives a χ^2 curve which in the region of the minimum is fitted with a fourth-order polynomial (Fig. 5 right). The position of the minimum of the polynomial, $m_{\mathrm{W}}^{\mathrm{min}}$, gives the best value of the W mass and the uncertainty $\sigma(m_{\mathrm{W}})$ is obtained from the values where $\chi^2 = \chi^2_{\mathrm{min}} + 1$. The mean value of $\sigma(m_{\mathrm{W}})$ for all ensembles are quoted as expected statistical uncertainties (see Fig. 6).

The expected statistical errors on the W mass using histogram fitting are comparable to those using the function fitting method. However, since the former exploits the complete missing mass distribution, it is more sensitive to potential biases from imperfect simulation of the roman pot detectors.

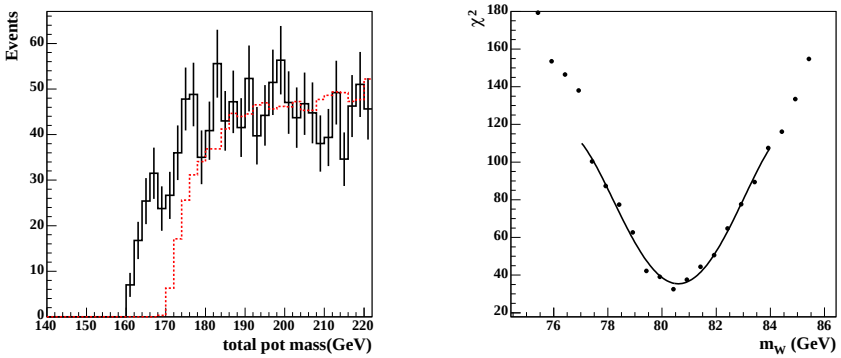

FIG. 5: Left: Example of the histogram-fitting method. We see the difference between the "data" sample (full histogram with error bars, $m_{\rm W} = 80.42$ GeV) and a reference histogram (dashed line, $m_{\rm W} = 85.42$ GeV). Right: Example of the χ^2 distribution in one ensemble.

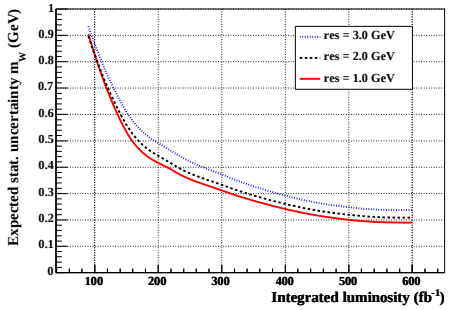

FIG. 6: Expected statistical precision of the W mass as a function of the integrated luminosity for various resolutions of the roman pot detectors using the histogram-fitting method.

V. CONCLUSION AND OUTLOOK

Recent work on DPE has essentially focused on the Higgs boson search in the exclusive channel. In view of the difficulties and uncertainties affecting this search [15], we highlight new aspects of double diffraction which complement the diffractive program at the LHC.

In particular, QED W pair production provides a certain source of interesting diffractive events. In this paper, we have advocated the interest of threshold scans in double photon exchange. This method may extend the physics program at the LHC. To illustrate its possibilities, we described in detail the W boson mass measurement. The precision of the W mass measurement is not competitive with other methods, but provides a very precise calibration of the roman pot detectors, since the cross sections and characteristics of this QED process are well under control. This method can be extended to any particle production via exclusive processes and was applied to SUSY particle production as an example [16].

Finally, W pair production in central diffraction gives access to the coupling of gauge bosons. Namely, as we mentioned already, W^+W^- production in two-photon exchange is robustly predicted within the Standard Model. Any anomalous coupling between the photon and the W will reveal itself in a modification of the production cross section, or by different angular distributions. Since the cross section of this process is proportional to the fourth] power of the photon-W coupling, a good sensitivity is expected. This study will be described in an incoming paper [17].

[1] K. Piotrzkowski, Phys. Rev. D **63** (2001) 071502.
[2] E. Papageorgiu, Phys. Lett. B **250**, 155 (1990).
[3] V. M. Budnev, A. N. Vall and V. V. Serebryakov, Yad. Fiz. **21**, 1033 (1975).
[4] T. Binoth, M. Ciccolini, N. Kauer and M. Kramer, arXiv:hep-ph/0503094.

[5] J. D. Bjorken, Phys. Rev. D **47**, (1993) 101; E. Gotsman, E. Levin and U. Maor, Phys. Lett. B **438** (1998), 229; A. B. Kaidalov, V. A. Khoze, A. D. Martin and M. G. Ryskin, Eur. Phys. J. C **21** (2001) 521; A. Bialas, 'Acta Phys. Polon. B **33** (2002) 2635; A. Bialas, R. Peschanski, 'Phys. Lett. B **575** (2003) 30.

[6] A. Donnachie, P. V. Landshoff, *Phys. Lett. B* **207** (1988) 319.

[7] V. A. Khoze, A. D. Martin and M. G. Ryskin, Eur. Phys. J. C **23**, 311 (2002)

[8] M. Boonekamp, T. Kucs, Comput. Phys. Commun. **167** (2005) 217.

[9] G. Corcella et al., JHEP **0101:010** (2001).

[10] J. Kalliopuska, T. Mäki, N. Marola, R. Orava, K. Österberg, M. Ottela, HIP-2003-11/EXP.

[11] M. G. Albrow and A. Rostovtsev [arXiv:hep-ph/0009336].

[12] CMSIM, fast simulation of the CMS detector, CMS Collab., Technical Design Report (1997);
TOTEM Collab., Technical Design Report, CERN/LHCC/99-7;
ATLFAST, fast simulation of the ATLAS detector, ATLAS Collab, Technical Design Report, CERN/LHC C/99-14.

[13] G. Abbiendi *et al.* [OPAL Collaboration], Eur. Phys. J. C **26**, 321 (2003) [arXiv:hep-ex/0203026].

[14] N. Gehrels, Astrophys. J. **303**, 336 (1986).

[15] M. Boonekamp, R. Peschanski and C. Royon, Nucl. Phys. B **669**, 277 (2003); M. Boonekamp, R. Peschanski and C. Royon, Phys. Lett. B **598**, 243 (2004); M. Boonekamp, R. Peschanski and C. Royon, Phys. Rev. Lett. **87**, 251806 (2001)

[16] M. Boonekamp, J. Cammin, S. Lavignac, R. Peschanski, C. Royon, Phys. Rev. D **73** (2006) 115011.

[17] M. Boonekamp, O.Kepka, R. Peschanski, C. Royon, in preparation.